International Journal of Advanced Geosciences, 14 (1) (2026) 20-29

International Journal of Advanced Geosciences

Website: www.sciencepubco.com/index.php/IJAG
https://doi.org/10.14419/hm2j5z48
Research paper

Morphometric Analysis of Subbasins Along The Basalt-Granite Contact in The South East Deccan Volcanic Province, India

Deepak Wable [1] *, Ramakant Kaplay [2], Udaykumar Sahu [3], Divyesh Vyas [1]

[1] School of Earth Sciences, Swami Ramanand Teerth Marathwada University, Nanded – 431 606, Maharashtra, INDIA
[2] Maharashtra National Law University, Mumbai – 400076, Maharashtra, INDIA
[3] Department of Geology, Toshniwal College of Arts, Commerce and Sciences, Sengaon, Hingoli – 431 542, Maharashtra, INDIA
**Corresponding author E-mail: deepak.wable78@gmail.com*

Received: October 29, 2025, Accepted: January 20, 2026, Published: January 24, 2026

Abstract

Morphometric analysis of drainage basins using remote sensing (RS) and GIS is an effective way to assess the influence of lithology and tectonics. In this paper, the authors evaluated lithostructural controls on the sub-basins along the contact between basalt and granite in the South East Deccan Volcanic Province (SEDVP) and the Eastern Dharwar Craton (EDC) margin. Thirty-six drainage sub-basins (mini- to micro-watersheds) located in basalt, granite, and along the basalt-granite contact were selected to assess the influence of lithology and structures (lineament, faults, etc.) on drainage morphology. Geological fieldwork was carried out along the basalt-granite contact within the 62 km stretch from Adampur, Biloli (MH), to Bhainsa (TS). Eleven profiles of basalt-granite contacts were reported, which are further referred to classify the sub-basins based on lithology, namely, Category I: sub-basins that are located in basalt, Category II: sub-basins partially located in basalt (Deccan traps) and granite (basement), and Category III: sub-basins that are located in granite. In morphometric analysis, we have calculated drainage density (Dd), stream frequency (Fs), elongation ratio (Re), and asymmetry factors (Af). The assessment of morphometric analysis and reported structures suggests that the (1) category I sub-basins are tectonically inactive, whereas category II and III sub-basins are tectonically moderately active. (2) Reported evidence of sub-surface tectonic activity expressed as 'minor faults' within the basement granite underlying the thin capping of basalt/basaltic soil is profoundly manifested in the sub-basins, which are corroborated by morphotectonic evidence.

Keywords: *Basalt-Granite Contact; Field Structures; Morphometric Analysis; Morphotectonics, SEDVP*

1. Introduction

Differential resistance of lithologies controls landform morphology and drainage network behaviour, whereas faults, fractures, shear zones, and lineaments may act as favoured pathways for stream network development. Rock heterogeneities and tectonics plays crucial role in the development and evolution of drainage patterns and in 'shaping' the drainage basin (Horton, 1934, 1942; Radhakrishna, 1992; Sinha-Roy, 2001; Pati et al., 2008; Singh & Srivastava, 2011). The role of lithology promptly reflects in local-scale drainage basins (Ngapna et al., 2018). To establish the influence of lithologies and tectonics on drainage basins, morphometric assessment of drainage basins with field investigations is extremely useful (Ritter, 1986; Prakash et al., 2017).

Few studies in the SEDVP region have been conducted to understand the response of the drainage basin to tectonics with the help of geomorphic indices (Re, Af, etc.). The elongation ratio and asymmetry factor values of the drainage basin studied at the Nanded region are in favour of active tectonics, which is further supported by deformation reported in quaternary sediments and recent microseismic activities (Kaplay et al., 2016). In addition, morphometric analysis of the Kayadhu river basin and Kinwat basins suggests that the region is moderately tectonically active (Kaplay et al., 2017b; Ghute and Babar, 2021).

In the south east of Nanded, near the study area, several lineaments (N, NNE, NE, NW, and E) were observed in granitoid and basalt that were further interpreted as faults, fractures, and shear zones (Banerjee et al., 2008, 2012). Further, a northwest-trending Kaddam fault/lineament with quaternary reactivation, as evidenced by Sangode et al. (2013 towards the NE of the study area (Fig. 1). Moreover, east-west strike-slip faults are reported from the basement granite of Kinwat (60 km NE from the present study) (Kaplay et al., 2017b). Further, Kaplay et al. (2021 documented minor faults, grabens, and boudins in granites just beneath the Deccan traps.

The drainage sub-basins of the study area are part of the Godavari River, and its tributaries (Manjra and Siddha), which flow over the basalt and granite (Fig. 1). The impacts of lithological variation (basalt and granites) and structural discontinuities (faults, fractures, lineament, etc.) may be manifested in these uniquely located sub-basins. Therefore, the present study aims to understand how contrasting lithologies

Copyright © Deepak Wable et al. This is an open access article distributed under the Creative Commons Attribution License, which permits unrestricted use, distribution, and reproduction in any medium, provided the original work is properly cited.

and structures control the drainage basin morphology. For that, we applied four important morphometric parameters, viz., drainage density (Dd), stream frequency (Fs), elongation ratio (Re), and asymmetry factors (Af). The main objective of this study is to evaluate the level of morphotectonic activity in the area along the basalt-granite contact.

2. Study Area

The study area is located 62 km south-east of the microseismically active Nanded area (Kaplay et al., 2014). The study area is a linear stretch along the contact of basalt and granite (Fig. 1c), which is partly located in basalt (SEDVP), partly in granite (EDC). The coordinates of the study area are Latitude: 18°40'40.28"N to 19°06'11.35"N and Longitude: 77°37'24.83"E to 77°57'55.07"E. Geographical distribution of the area is 894.40 km^2, some part located in Biloli, Degloor, and Bhokar tehsils of Nanded district (Maharashtra) and some in Bhainsa mandal of Nirmal district (Telangana). Geologically, the area comprises Deccan basalt and Archean basement granite. Along the basalt-granite contact, thin, weathered basalt overlies pink to grey coarse-grained weathered granites. The granites are intruded by quartz-feldspathic/quartz veins and basic intrusions. The geological structures and vertical litho-contact of basalt and granite were reported from 11 sites (a,b,…, k; Fig. 1 and Table 3). Contact is typically transitional, i.e. lack of sharp distinction between basalt and granite except at Adampur (a) and Bhainsa (k) sites, where the contact is sharp (Table 3).

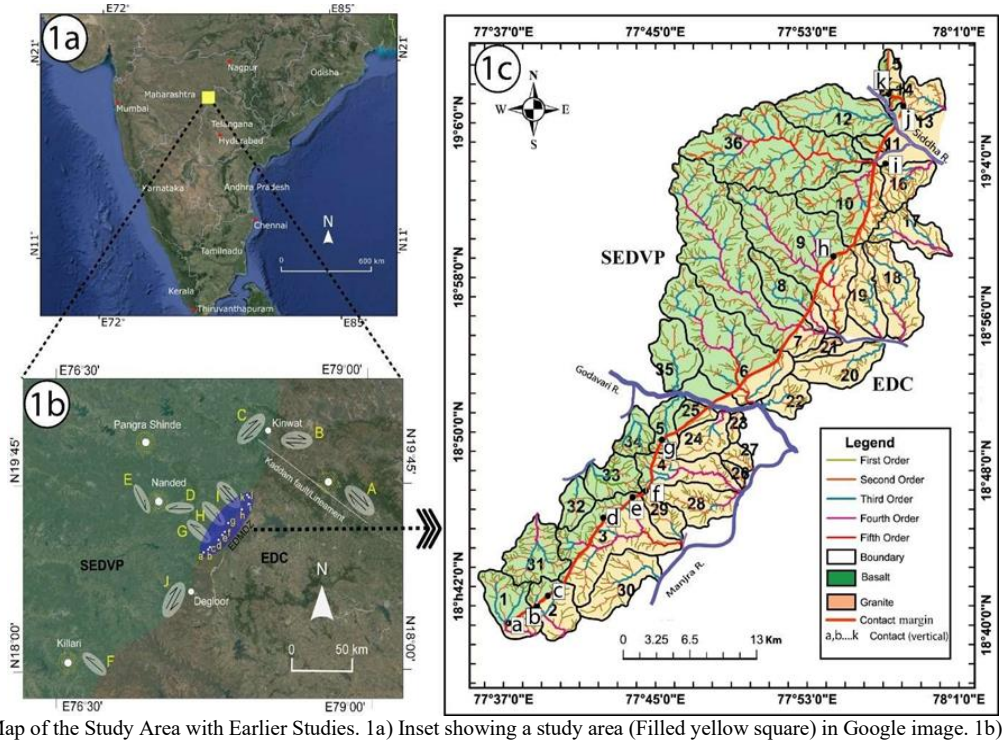


Fig. 1: Location Map of the Study Area with Earlier Studies. 1a) Inset showing a study area (Filled yellow square) in Google image. 1b) Magnified view of the study area graphically showing the earlier works in the region. Green shaded area – SEDVP, unshaded area – EDC. Transparent blue ellipse – denoting the approximate extent of East Dharwar Margin Deformation Zone (EDMDZ) (After Kaplay et al., 2021). White dotted line – Kaddam Fault/Lineament. Summary of recent work from the SEDVP – EDC margin: 'A', 'B', 'C', 'E', 'F', 'G', 'H', 'I', and 'J' in and around the Nanded. 'A' – NW-SE strike-slip faults near Kaddam (Sangode et al., 2012); 'B' – strike-slip faults with east west trend in granites near Kinwat (Kaplay et al., 2017b, 2019); 'C' – Northeast trending strike-slip faults in granites northwest of Kinwat; 'D' – west verging thrusts in Deccan Trap (DT) in Micro-Seismically Active Nanded (Kaplay et al., 2013); 'E' – steeply dipping normal faults in (DT) in Nanded (Kaplay et al., 2017a); 'F'- 'Slow-deforming non-rifted zone' (Intra-cratonic seismicity) (Rajendran et al., 1986); 'G', 'H' and 'I': 'G' – NW-SE reverse faults, 'H' – normal faults and 'I' – northwest trending strike-slip faults (Kaplay et al., 2021); 'J'- NW-SE strike-slip fault in granitoids Babar et al., 2019. White circles with dotted yellow rims – recent seismicity/micro-seismicity, 'A', 'B', 'C', 'D', 'E', 'F', 'G', 'H', 'I', 'J', and 'K' are the basalt-granite contacts of the present study. 1c Map showing drainage sub-basins of the area. Red line – basalt-granite contact.

3. Methodology

The sub-basins of the study area were divided into three categories based on their location in basalt, granite, and across the basalt-granite contact. Geological fieldwork was carried out to mark the basalt-granite contact and find the structures (faults, etc.) in rock along the road sections, quarries, and construction sites. Reported minor structures such as faults/offsets in pegmatite veins in granite underlying the Deccan basalt. The survey of India (SoI) toposheets (56F/10, 56F/13, 56F/14, and 56E/16) were scanned, geo-referenced, and onscreen digitization of drainage sub-basins was done in QGIS software. In this study, a total of 36 drainage sub-basins were extracted for morphometric analysis, which were further grouped into three categories: Category I: sub-basins located in the basalt (Deccan trap), Category II: sub-basins partially located in basalt and granite (basements), and Category III: sub-basins located in granite (Table 1, Fig. 1). Sub-basin categorisation facilitate comparative assessment of the influence of different lithologies and structurally controlled terrain on basin morphometry. Morphometric parameters such as drainage density (Dd), stream frequency (Fs), asymmetry factor (Af), and elongation ratio (Re) were calculated (Table 3) and later employed to assess the impacts of lithostructural controls on drainage sub-basins of the study area. Drainage analysis and stream ordering were carried out as per Horton's (1945) and Strahler's (1964) schemes.

Table 1: Three Categories of Drainage Sub-Basins of the Study Area

Category I		Category II		Category III	
Name	Sub-basin code	Name	Sub-basin code	Name	Sub-basin code
Pangri	12	Adampur	1	Kumsara	16
Bamni	31	Muthnyal	2	Karegaon	17
Chinchola	32	Pokharni	3	Vitholi	18
Kondalpur	33	Kundalwadi	4	Pedda	19
Daur	34	Pimpalgaon	5	Bedereli	20
Patoda	35	Dharmabad	6	Bedereli (Kh.)	21
Elegaon	36	Labdi	7	Rampur	22
		Dhondapur	8	Makli	23
		Mudhol	9	Karhala	24
		Degam	10	Jagni	26
		Wadgaon	11	Hugunda	27
		Pipri	13	Machnur	28
		Bhainsa	14	Bolegaon	30
		Mirzapur	15		
		Selgaon	25		
		Sultanpur	29		
Total	**7**		**16**		**13**

The sub-basin is named after a village/town located within the sub-basin.

Table 2: Morphometric Parameters Calculated in the Present Study

Parameters	Formula	References
Stream number (N_u)	Total number of streams of a given order within each basin boundary	Strahler (1952)
Stream order (S_u)	Hierarchical rank of stream/tributaries	Strahler (1952)
Stream length (L_u)	Total length of the stream	Horton (1945)
Drainage density (D_d)	$D_d=\Sigma L_u/A$ L_u=Total stream length of all orders A = Area	Horton (1932, 1945)
Stream frequency (F_s)	$F_s=\Sigma Nu/A$ N_u=Total number of streams of all orders A = Area of basin	Horton (1932, 1945)
Elongation ratio (R_c)	$R_c=2(\sqrt{A}/\pi)/L_b$ A = Area of basin L_b=Basin length π = 3.14	Schumm (1956)
Basin asymmetry (A_f)	Af =100(Ar/At) Ar = Area of the right (facing downstream) of the mainstream At = total area of the basin	Molin et al., (2004)

Table 3: Types of Contact (Basalt-Granite) and Deformations Reported from Associated Drainage Sub-Basins

Site name	Contact site	Sub-basin code.	Deformation	Contact type
Adampur	a	1	Not reported	Sharp
Muthnyal	b	2	Reported	Transitional
Minki	c	2	Not reported	Infratrappean limestone
Phokarni	d	3	Not reported	Transitional
Biloli	e	3	Reported	Basaltic soil
Biloli	f	29	Not reported	Transitional
Pimplagaon	g	5	Reported	Thin soil cap
Mudhol	h	9	Not reported	Infratrappean limestone
Degam	i	16	Reported	Thin soil capping
Bhainsa	j	14	Reported	Backed sediment stuff
Bhainsa	k	15	Not reported	Sharp

4. Field Characteristics of Basalt-Granite Contact

Eleven profiles of basalt-granite contact have been identified and designated as ‘a’ to ‘k’ (Fig. 1 and Table 3) out of which nine profiles (‘b’ to ‘j’) shows transitional contact, whereas, two profiles (‘a’ and ‘k’) shows sharp contact (Table 3) along the margin of South East Deccan Volcanic Province (SEDVP) and eastern Dharwar Craton (EDC). Due to intense physicochemical weathering induced by meteoritic water contact between basalt and granite transitional, i.e., gradual variation in lithology from basalt to granite without a sharp distinction between them. The contact comprises weathered granite and basalt with occasional thin capping of basaltic soil (site ‘& ‘e’) with varying thickness of basalt from 1 to 5 meters. Infratrappean limestone (site c & h) and red tachylitic basalt (site g) are sandwiched between basalt and granite, whereas variation in colour of weathered rocks from green, violet to reddish is observed, which indicates different intensity of baking of basaltic eruption over the older granite (site ‘d’ &‘f’). The soil and weathered basalt appeared reddish in colour due to oxidation processes, and the shallow sub-surface granites are pink coloured due to high content of alkali feldspar.

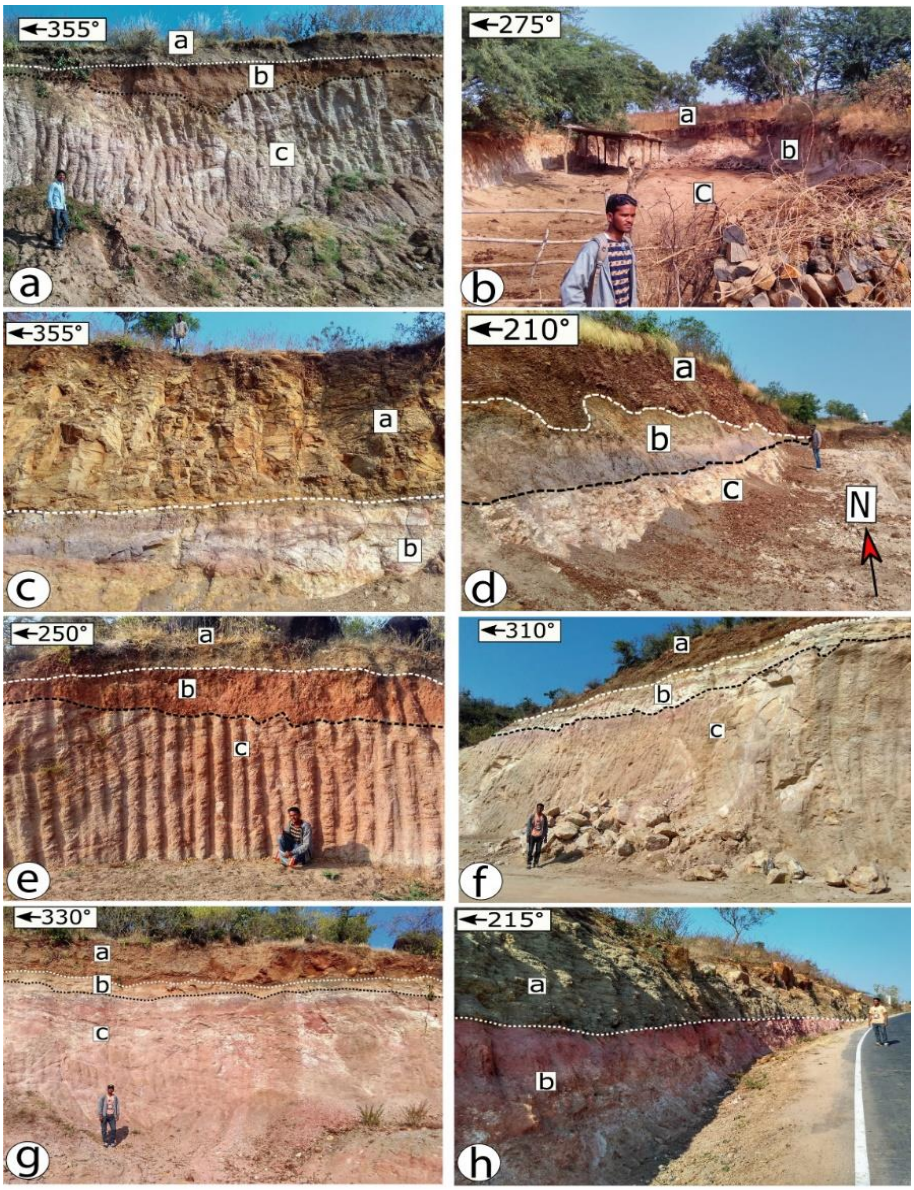


Fig. 2: Basalt-granites contacts (vertical sections). a) Weathered basaltic soil cover 'a' on the weathered granite 'c', is separated by 'basalt-granite' transition 'b' (Loc: site b (Muthnyal) 18º40′34″N, 77º38′21″E); b) Basalt 'a' and underlying granite 'c' is separated by limestone infratrappean bed 'b' (Loc: site c (Minki) 18º41'34.38"N, 77º39'12.30"E); c) Granitic rock 'b' overlain by weathered and jointed massive basalt 'a' (Loc: site d (Pokharni) 18º45′N, 77º41′E); d) Undulating basalt 'a' and granite 'c' contact with basalt - granite' transition 'b' (Loc: site f (Biloli) 18º48′27″N, 77º46′02″E); e) Contact is separated by thick red bole 'b'. (Loc: site g (Pimpalgaon) 18º58′27″N, 77º54′45″E); F) in a quarry limestone bed 'b' is sandwiched between weathered basalt 'a' and pink granite 'c' (Loc: site h (Mudhol) 18º58'39.31"N, 77º53'49.23"E); g) Vertical profile showing transitional contact 'c' (Loc: site J (Bhainsa) 18º07′16″N, 77º57′55″E) and h) in road-cutting section observed a distinct contact of basalt 'a' is directly overlain to granite 'b', dotted white line – contact.

5. Field Structures

Structural deformations reported from granites underlying basalt are mostly 'minor faults' in pegmatite veins. From granites of profile 'b', 'e', 'g', 'i', and 'j', shows brittle and ductile deformations (Fig. 6), no structures/deformation observed in basalt so far. At site 'b', a 25cm thick pegmatite vein showing a normal fault with net slip 7.6cm (Fig.3a). A low angle (15º) normal fault is reported from pink granite (Fig.3b). At site 'e', a bifurcated pegmatite dyke showing a reverse fault with 45º dip towards southwest (Fig.3c). At site 'g', 'older' pegmatite vein'P1' get faulted (F1) with a 25cm slip; subsequently, 'P1' got another offset at 'F2', which later intruded with 'younger' 3cm thick pegmatite vein 'P2' (Fig. 3d). Site 'i' showing that pegmatite vein 'P1' intruded in amphibole-rich granite-gneiss got displaced by a normal fault with net slip of 10.5cm, later fault plane accommodated with 'younger' pegmatite vein 'P2' (Fig. 3e). At site 'j', in weathered amphibole-rich granite, a horizontal offset (dotted white line) in pegmatite dyke 'P' with a slip of 13cm (Fig. 3f). Pegmatite, epidotic veins, and quartzo-feldspathic veins/dykes with minor faults are common in granite along the contact.

These brittle deformations are restricted to the granites, whereas no such deformations are reported in the overlying basalt. This study aims to evaluate the influence of subsurface tectonics on the drainage sub-basins located along the basalt–granite contact through morphotectonic assessment.

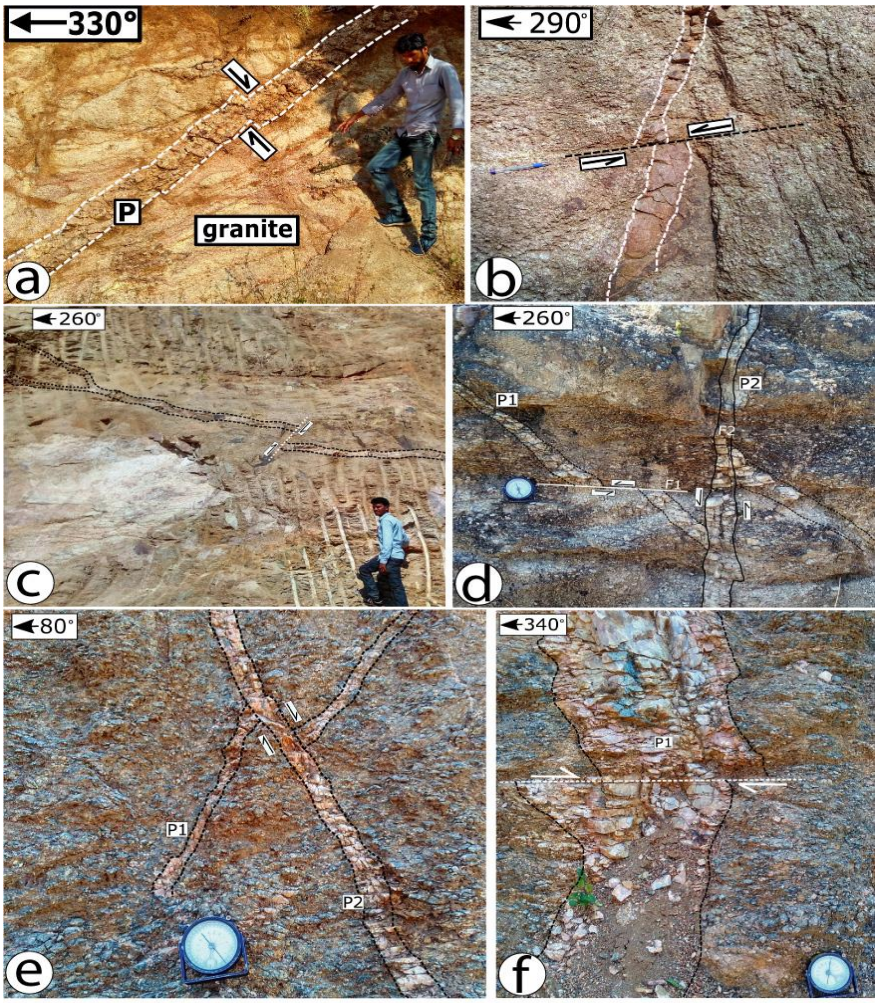


Fig. 3: Field structures reported from granites just underneath the basalt. a) A 27cm thick pegmatite vein 'P' showing offset (7.6cm) with dip of 36º towards NW, b) A low angle normal fault (dotted black line) in quartzo-feldspathic vein (dotted white line) with dips 15º/SW) in granite (Fig. '3a' and '3b'from Loc: site b (Muthnyal) 18º40′34″N, 77º38′21″E); c) A bifurcated pegmatite vein (dotted black lines) shows reverse offset with dip 45º SW (white lines) (Loc: site e (Biloli) 18º46′40″N, 77º42′41″E); d) Pegmatite veins 'P1' and 'P2' shows offset 'F1' and 'F2' (Loc: site g (Pimpalgaon) 18º55′13″N, 77º51′46″E). White lines – fault planes; e) Offset (9cm slip with dip 50ºW) in cross-cutting quartzo-feldspathic vein 'P1', fault plane with younger relatively pegmatite vein 'P2'; f) Vertical pegmatite vein 'P1' with horizontal offset (dotted white line – offset plane (Loc: site i (Degam) 19º04'8.18"N, 77º56'55.71"E).

6. Results

Drainage density (Dd), stream frequency (Fs), elongation ratio (Re), and asymmetry factors (Af) were calculated for the sub-basins of all three categories. Dd and Fs suggest the impact of lithology (granite and basalt) on drainage sub-basins, whereas Re and Af evidenced the sub-basins' tectonics. The parameters and their tectonic aspects have been examined and discussed in relation to their relevant morphotectonic significance.

6.1. Drainage density (Dd)

The value of Average Dd for category I, II, and III sub-basins is 1.87 (Table 4), 1.83 (Table 5), and 1.69 (Table 6), respectively. These values significantly decrease from basalt to granite. Low value of Dd (1.69) of the category III sub-basins suggests resistant lithology or highly permeable subsoil materials (Horton, 1932; Sangode et al., 2013). Whereas, values of high Dd (1.87) for category I sub-basins are favoured in regions of weakly impermeable basaltic soil compared to granitic soil with sparse vegetation cover (Strahler, 1964). Further, the average of Dd for category II sub-basins (1.83) is intermediate between category I and III sub-basins, which may be due to partial location of sub-basins in basalt and granite.

Table 4: Morphometric analysis of category I sub-basins

S. No.	Sub basin code	Highest order of sub-basin	N_u	L_u (km)	A (Km^2)	D_d	F_s	R_e	A_f
1	33	Third order	38	33.08	16.62	1.99	2.29	0.86	51.75
2	35	Third order	18	25.04	21.44	1.17	0.84	0.75	52.14
3	12	Third order	54	65.54	35.55	1.84	1.52	0.60	51.15
4	31	Fourth order	78	60.91	25.08	2.43	3.11	0.80	39.04
5	32	Fourth order	10	12.90	10.68	1.21	0.94	0.69	47.70
6	36	Fourth order	231	176.91	88.81	1.99	2.60	0.59	52.11
7	34	Fourth order	36	28.05	11.43	2.45	3.15	0.76	42.18
Average						**1.87**	**2.06**	**0.72**	**48.01**

N_u total numbers of stream of all orders; L_u total stream length of all orders; A area of sub-basins; D_d drainage density; F_s stream frequency; R_e elongation ratio, and A_f asymmetry factor

Table 5: Morphometric analysis of category II sub-basins

S. No.	Sub-basin code	Highest order of sub-basin	N_u	L_u (km)	A (Km^2)	D_d	F_s	R_e	A_f
1	1	Fourth order	45	44.60	23.27	1.92	1.93	0.69	25.78
2	2*	Fourth order	39	42.17	20.30	2.08	1.92	0.80	30.36
3	3*	Fifth order	130	112.65	56.77	1.98	2.29	0.70	27.43
4	4	Fourth order	46	41.58	24.30	1.71	1.89	0.53	34.32
5	5*	Third order	29	25.40	11.94	2.13	2.43	0.65	46.60
6	6	Fifth order	128	114.33	71.39	1.60	1.79	0.64	35.56
7	8	Fourth order	49	38.26	20.79	1.84	2.36	0.48	43.03
8	10	Fifth order	106	77.70	37.39	2.08	2.83	0.81	37.14
9	15	Second order	7	10.25	7.22	1.42	0.97	0.66	28.13
10	13	Fourth order	35	26.03	12.09	2.15	2.89	0.85	43.53
11	9*	First order	189	159.37	79.29	2.01	2.38	0.57	34.83
12	25	Third order	7	8.88	7.83	1.13	0.89	0.81	-
13	29*	Third order	18	17.29	10.82	1.60	1.66	0.62	39.12
14	11	Second order	8	6.05	3.60	1.68	2.22	0.71	37.27
15	14*	Second order	5	4.13	2.00	2.07	2.50	0.65	39.81
16	7	Fourth order	233	199.49	101.81	1.96	2.29	0.51	49.60
Average						**1.83**	**2.07**	**0.67**	**36.83**

*Deformation reported from granite underneath the basalt

Table 6: Morphometric Analysis of Category III Sub-Basins

S. No.	Sub-basin code	Highest order of sub-basin	N_u	L_u (km)	A (Km^2)	D_d	F_s	R_e	A_f
1	28	Third order	43	37.94	21.75	1.74	1.98	0.63	44.41
2	16 *	Fourth order	46	41.70	16.09	2.59	2.86	0.72	34.50
3	26	Second order	4	4.53	2.72	1.67	1.47	0.56	-
4	27	Second order	9	9.43	5.17	1.82	1.74	0.76	38.62
5	22	Third order	19	20.84	11.99	1.74	1.58	0.81	44.32
6	30	Third Order	30	38.42	26.29	1.46	1.14	0.64	36.54
7	17	Fourth Order	50	41.94	18.58	2.26	2.69	0.66	25.74
8	19	Fourth order	37	32.66	19.17	1.70	1.93	0.53	63.93
9	18	Fourth order	62	58.66	30.54	1.92	2.03	0.62	48.85
10	20	Third order	34	32.35	21.67	1.49	1.57	0.57	65.49
11	21	Second order	3	5.46	4.14	1.32	0.72	0.47	-
12	24	Fourth order	21	20.54	15.87	1.29	1.32	0.64	50.29
13	23	Second order	3	3.39	3.18	1.07	0.94	0.65	-
14	18	Fourth order	62	58.66	30.54	1.92	2.03	0.62	48.85
15	20	Third order	34	32.35	21.67	1.49	1.57	0.57	65.49
Average						**1.69**	**1.70**	**0.63**	**47.25**

6.2. Stream frequency (Fs)

Fs (1 to 3.5) indicates stream or channel segments being controlled by the fractures (Horton, 1932, 1945; Melton, 1958). Fs (Horton, 1932) values positively correlate with the values of Dd. The average value of Fs for category I, II, and III sub-basins is 2.06, 2.07, and 1.70, respectively. The average Fs is similar for sub-basins of categories I and II, but significantly less (1.70) for the category III sub-basins (Table 4, 5, and 6).

6.3. Elongation ratio (Re)

Re is one of the indices used for determining the shape of a drainage basin, i.e., elongated or circular. Re usually varies from 0.6 to 1.0 over a wide range of climatic and geological conditions, near 1.0 is typical for the region with very low relief, whereas, for strong relief and steep ground slopes, it ranges from 0.6 to 0.8 (Strahler, 1964). Tectonic control on a drainage basin is reflected by the elongated shape of the basin as a whole. Re value ranges from < 0.50, through 0.50 - 0.75, and > 0.75 for tectonically active, slightly active, and inactive basins, respectively (Cueong & Zuchiewicz, 2001). In the study area, the average Re ratio for category I, II, and III sub-basins is 0.72 (Table 4), 0.67 (Table 5), and 0.63 (Table 6), respectively. Re is relatively lower for category III sub-basins than for category I and II sub-basins. These Re values may indicate that category I Sub-basins are tectonically inactive and category II and III sub-basins are moderately tectonically active (Cueong & Zuchiewicz, 2001).

6.4. The asymmetry factor (Af)

Asymmetry factor (Af) is used to assess the lateral tilting (tectonic tilting) of a drainage basin (Hare & Gardner, 1985; Cox et al., 2001; Cueong & Zuchiewicz, 200; Singh & Srivastava, 2011). Due to active tectonics or lithological controls, Af >50 implies basin tilt to the left, whereas Af <50 implies basin tilt to the right (Cox et al., 2001). For the category I sub-basins, the Af values show relatively less significant variation, ranging from 39.04 to 52.1 (Table 4), compared to the Af values for category II and III sub-basins. The category II sub-basins show Af value ranges from 25.78 to 49.60 (Table 5). Further, Af for category III sub-basins ranges from 25.74 to 65.49 (Table 6), suggesting significant tectonic influence (Keller & Pinter, 1996; Molin et al., 2004).

7. Discussion

Morphometric analysis was done for all sub-basins, and a suitable classification was applied for comparative assessment of morphometric parameters. The sub-basins of the study area are spread over the granitic and basaltic terrains. Geological structures corroborate that morphotectonic indices can be used to deduce the influence of the structures on the development of the drainage network and rivers flowing

over the basalt and granite. Noteworthy link between morphotectonics and deformation structures is reflected in the form of drainage development in the study area. The results of the morphometric analysis and their significance to morphotectonics have been discussed below.

Streams considered for this study belong to the third to fifth orders. Streams showing the distinct 'sharp knee-bend', i.e., linear course of streams, takes right angle turns (Fig. 4), deviating from the typical sinuous flow pattern. These anomalous behaviours are believed to be indicative of strong influence faults in the area (Twidale, 2004), while the regional drainage pattern of the area is mainly dendritic along with occasional sub-parallel and trellis patterns (Fig. 4). In the northern side of study area higher order stream of sub-basins profoundly oriented in NW- SE direction (Fig. 6). These streams are aligned with Kaddam lineament (Sangode et al., 2013) and Kinwat lineament (NW extension of Kaddam lineament) and E-W strike fault reported at Kinwat from granites (Kaplay et al., 2017b, 2019). It suggests that higher-order streams may flow over the concealed fault in the granites of the study area. Whereas, middle to low order streams make dendritic drainage with occasional trellis and sub-parallel drainage pattern (Fig. 4). In addition, differences in trend of fault orientation indicate the heterogeneity in fault regime at the local scale (Kaplay et al., 2019), which is manifested in the form of drainage pattern of middle and lower order streams (Fig. 4). Higher order streams of sub-basins 4, 9, 10, 30, and 36 show relatively straight courses with right-angle turn (sharp knee-bend). Notably, these sub-basins are either located in granites or across the contact but not in the basalt. Reported structures from the granites along the contact confirm the presence of subsurface fractures/faults in the granites beneath the basalt, which act as a prerequisite to control the drainage development in sub-basins. Furthermore, many sub-basins (Table 7) show an evident variation in the number of streams on either side of the mainstream. This may be attributed to the 'asymmetry of the basin' (Keller, 1996; Rawat et al., 2022; Cox et al., 2001). Most of the sub-basins tilt towards the SW direction (Fig. 6). Ten sub-basins display significant distribution of streams on either side of the trunk stream (Table 7 & Fig. 5). This characteristic feature demonstrates asymmetry, indicating the 'tilting of the basin' (Molin et al., 2004).

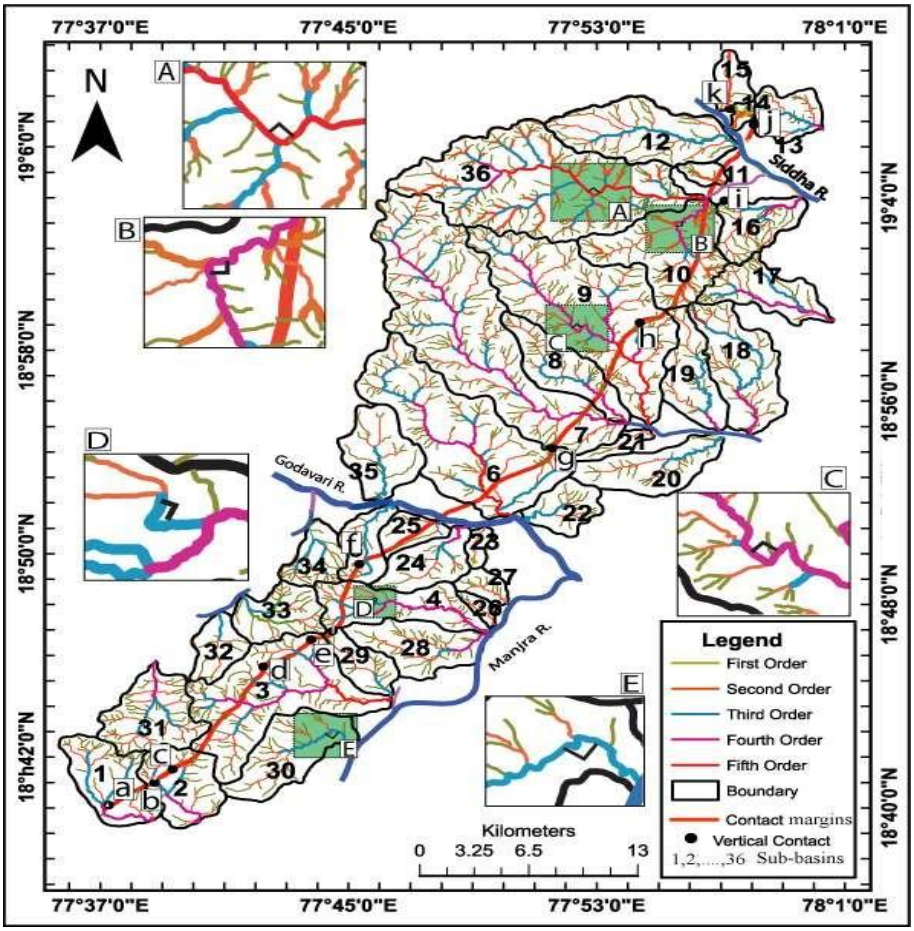


Fig. 4: Study area showing sub-basins of the Godavari River and its tributaries, the Manjra and Siddha Rivers. Magnified view showed in inset A, B, C, D, and E showing 'Sharp knee bend' in stream course reported from sub-basins 4, 9, 10, 30, and 36. Small letters – contact sites; capital letters with green shaded boxes – sharp knee bend in maps of drainage.

Table 7: Asymmetry Factor of the Sub-Basins

Sub-basin code	Deformation	Lithology	No. of streams right to the main stream	No. of streams left to main stream
1	Reported	Basalt and granite	2	37
2	Reported	Basalt and granite	11	19
3	Reported	Basalt and granite	25	78
4	Not reported	Basalt and granite	12	32
5	Reported	Basalt and granite	2	17
16	Reported	Granite	34	7
17	Not reported	Granite	12	31
20	Not reported	Granite	21	10
27	Not reported	Granite	1	7
30	Not reported	Granite	3	23

'Right' and 'left' to main stream within the sub-basin when facing downstream direction.

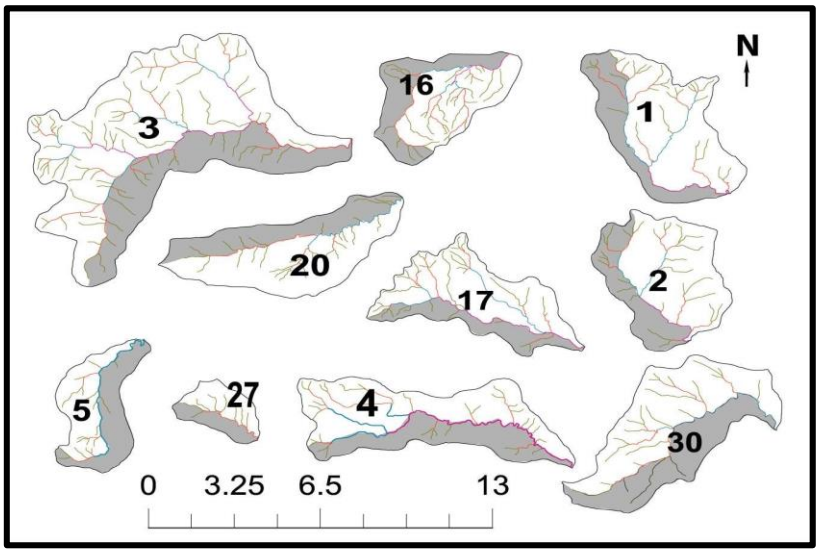


Fig. 5: The sub-basins (1, 2, 3, 4, 5, 16, 17, 20, 27, and 30) showing the significant unequal distribution of stream on either side of the trunk (master) stream of the sub-basin. Grey-shaded area – the right or left bank of the sub-basin with the minimum number of streams compared to the other half.

The morphometric analysis was carried out for each category separately, which will help in the comparative assessment of sub-basin morphotectonics. Firstly, category I sub-basins are flowing over the basalt (green-shaded area in the map) toward the southeast direction (Fig. 1). Category I sub-basins are part of the Godavari River and its tributaries, Siddha and Manjra rivers. The average value of Dd (1.87) for these sub-basins indicates less permeable basaltic soil cover with low-to-moderate relief. In contrast, the average value of Fs (2.06), which is positively correlated with Dd, suggests that the area has a higher frequency of stream development in basalt compared to granite. The average of Re (0.72) suggests that the category I sub-basins are, to some extent, tectonically inactive, which is supported by the insignificant variation in the Af (39-52) (Table 4). In support of that, no structures (faults, folds, etc.) have been reported from the basalt.
Secondly, category II sub-basins with the fifth-highest order flow in both basaltic and granitic terrain (Table 5) (Fig. 1). Stream flows from northwest towards southeast direction. The average Dd (1.83) and Fs (2.07) suggest a close relation with category I values. Dd and Fs may be influenced by vegetation, rock type, etc. (Villela & Mettos, 1975). Category II sub-basins flow over weathered basalt and granitic terrain. The basaltic and granitic soil may modify the soil infiltration and run-off properties, which may reflect in Dd and Fs. In contrast, average Re (0.67) and major variation in range of Af (26 - 49) suggest that these sub-basins are 'moderately tectonically active', which is further advocated by the reported structures (faults in granites) along the contact. Sub-basins show dominant 'tilting' towards the south-west direction (Fig. 6). Implicitly, the value of Dd and Fs seems to be more inclined towards the values of category I sub-basins. Meanwhile, the Re and Af of category I sub-basins are very close to the values of category III sub-basins. Therefore, this strongly implies that sub-surface tectonics may be manifested in the sub-basins.
Fifteen sub-basins with the highest fourth order are present in category III, which flow over the granitic terrain (Table 6). The average Dd (1.69) and Fs (1.70) suggest that granitic rocks are relatively more permeable than basalts, particularly in high-vegetation coves with low relief. Average Re (0.63) suggests that the category III sub-basins are 'moderately tectonically active'. In addition to that, Af (26-65) shows the tilting of sub-basins on either side of the mainstream. The Re values align with the Kinwat basin, which is moderately tectonically active; however, the Af shows slight variation (45-55) (Kaplay et al., 2019). A detailed hydrogeological and geophysical research work on concealed/hidden faults and their impact on groundwater quality and quality, in these lithologically controlled study areas, would be much required.

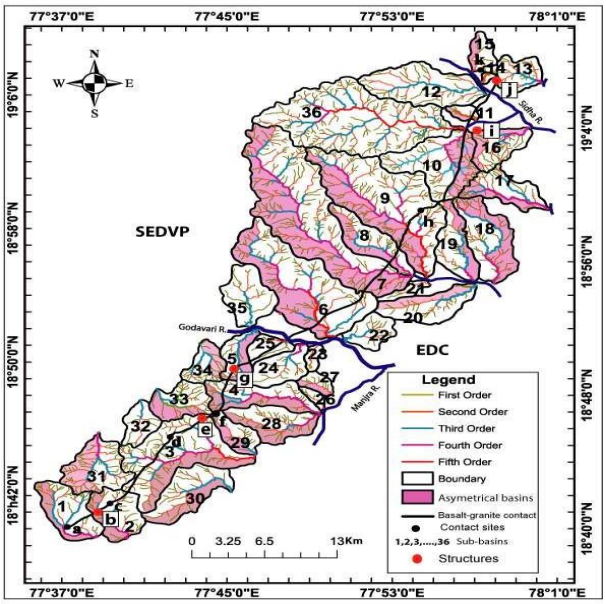


Fig. 6: Map showing the drainage basin asymmetry. The pink shaded part of the sub-basin with the minimum area and streams, while red-filled circles are the contact sites where deformations are reported.

Deformation structures primarily in the granites underlying the basalt in the study area (Kaplay et al., 2021) and from basalt around the Nanded city (Kaplay et al., 2021) are reported, which are located 62 km northwest of the study area. Strike-slip faults, thrust faults, horst-graben structures, boudinage, folding, and shearing in veins are reported in the granites of the study area. All these structures were confined to granites, and no deformations were reported from the overlying basalt. Average Re for category II (0.67) and III (0.63) sub-basins suggest 'tectonic tilting' (Hare & Gardner, 1985; Cox et al., 2001; Molin et al., 2004) (Table 5 & 6). Morphometric analysis of the study area suggest that significant impact of past tectonic activity on basin morphology. The structures reported at the outcrop scale further reinforce this finding. However, the study area has reported no micro-seismicity or seismic activity. Structures from basalt, quaternary deposits, or recent alluvium have yet to be reported in the study area. The nearest micro-seismicity is ~ 62 km from the study area in the Nanded region (Kaplay et al., 2017b). Additionally, micro-seismicity has been reported along the Kinwat Lineament (KL), approximately 63 km from the study area.

8. Conclusions

The study on morphotectonic indices for the selected drainage basins lying within basalt, basalt-granite contact, and in granites infers the influence of lithology and structures on basin morphology and stream development. The sharp knee bends in the course of streams of the sub-basins in the area might have developed under the influence of local-scale fractures/faults. To understand these, we determined Dd, Fs, Re, and Af for category I, II, and III sub-basins. Inferences drawn from the morphometric analysis are -

1) Category I sub-basins have average Dd (1.8) and Fs (2.06) that are relatively higher than Category II and III sub-basins, which suggests that basaltic soil is less resistant and has low permeability, and is barely covered with vegetation. Furthermore, the average Re (0.72) and range of Af (39 - 52) values suggest that the sub-basins are tectonically inactive and with insignificant tilt.
2) Category II sub-basins flow partly in the basalt and partly in the granites. The mean Dd (1.83) and Fs (2.07) suggest a drainage network modified with lithological heterogeneity. Furthermore, mean Re (0.67) and range of Af (26 - 49) of sub-basins suggest that sub-basins are elongated, moderately tectonically active, and tilted. Soil signatures of Dd and Fs for category II are closely related to category I, but Re and Af values lean towards category III, which suggests that Category II is moderately tectonically active. Reported structures confirm that the sub-surface basement tectonics may influence the drainage morphology even beneath thick basaltic cover.
3) Category III sub-basins in granite, the average Dd (1.69) and Fs (1.70) shows rock is resistant and highly permeable, weathered and jointed. In addition, average Re (0.63) and range of Af (26 - 65) suggest that category III sub-basins are elongated, moderately tectonically active, and tilted.
4) The sub-basin of category I, which flows on basalt are tectonically inactive, and no structural deformation has been reported. Meanwhile, the sub-basins of categories II and III are moderately tectonically active, as evidenced by structures (folds and faults) reported from granite below the basalt. The dominant 'tilt' direction is southwest.

Acknowledgement

The authors express their gratitude to the Director, School of Earth Sciences, Swami Ramanand Teerth Marathwada University, Nanded, Maharashtra, India, for providing the necessary facilities and support during this work.

Authors' Contribution

Deepak Wable: Field work, Data acquisition, Data Interpretation, Writing-original draft; Ramakant Kaplay: Conceptualization and supervision; Divyesh Vyas: Field work, Digitisation, Map preparation; Uday Sahu: editing, review, and supervision.

Conflict of Interest

The authors declare that they have no known competing financial interests or personal relationships that could have appeared to influence the work reported in this paper.

References

[1] Babar, M. D., Kaplay, R. D., Mukherjee, S., Mahato, S., & Gurav, C. (2019). NE-SW strike- slip fault in the granitoid from the margin of the South East Dharwar Craton, Degloor, Nanded district, Maharashtra, India. Tectonics and Structural Geology: Indian Context, 115- 134. https://doi.org/10.1007/978-3-319-99341-6_5

[2] Banerjee, R., Jain, S. K., & Shivkumar, K. (2008). Geochemistry and petrogenesis of uraninite-bearing granitoids and radioactive phosphatic cherty cataclasite of Thadiasoli area, Nanded district, Maharashtra. Memoirs of Geological Society of India, 73, 55–84.

[3] Banerjee, R., Shivkumar, K., Maithani, P. B. (2012). Major and trace element geochemistry of palaeoproterozoic Nanded district, Maharashtra: geodynamic and petrogenetic implications. Journal of Applied Geochemistry 26–58

[4] Cox, R. T., Van Arsdale, R. B., & Harris, J. B. (2001). Identification of possible Quaternary deformation in the northeastern Mississippi Embayment using quantitative geomorphic analysis of drainage-basin asymmetry. *Geological Society of America Bulletin*, *113*(5), 615-624. https://doi.org/10.1130/0016-7606(2001)113<0615:IOPQDI>2.0.CO;2

[5] Cuong, N. Q., & Zuchiewicz, W. A. (2001). Morphotectonic properties of the Lo river fault near Tam Dao in North Vietnam. *Natural Hazards and Earth System Sciences*, *1*(1/2), 15-22. https://doi.org/10.5194/nhess-1-15-2001

[6] Ghute, B. B., & Babar, S. M. (2021). Morphotectonics of Kayadhu River Basin in Washim-Hingoli-Nanded Districts, Maharashtra: A Spatial Analysis. Geological and Geo-Environmental Processes on Earth, 305-313. https://doi.org/10.1007/978-981-16-4122-0_20

[7] Hare, P. W., & Gardner, T. W. (1985). Geomorphic indicators of vertical neotectonism along converging plate margins, Nicoya Peninsula, Costa Rica. *Tectonic geomorphology*, *4*, 75-104.

[8] Horton RE (1932) Drainage-basin characteristics. Eos, Transactions American Geophysical Union, 13(1), 350–361. https://doi.org/10.1029/TR013i001p00350

[9] Horton, R. E. (1945). Erosional development of streams and their drainage basins; hydrophysical approach to quantitative morphology. Geological society of America bulletin, 56(3), 275-370. https://doi.org/10.1130/0016-7606(1945)56[275:EDOSAT]2.0.CO;2

[10] Kaplay, R. D., Babar, M. D., Mukherjee, S., & Kumar, T. V. (2017a). Morphotectonic expression of geological structures in the eastern part of the South East Deccan Volcanic Province (around Nanded, Maharashtra, India). Geological Society, London, Special Publications, 445(1), 317-335. https://doi.org/10.1144/SP445.12
[11] Kaplay, R. D., Babar, M. D., Mukherjee, S., Wable, D., & Pisal, K. (2021). Granitic Rocks Underlying Deccan Trap Along the Margin of East Dharwar Craton, Mutnyal (Maharashtra)—Bhaisa (Telangana), India—General Descriptionand Deformation. Structural Geology and Tectonics Field Guidebook—Volume 1, 599-620. https://doi.org/10.1007/978-3-030-60143-0_20.
[12] Kaplay, R. D., Babar, M., Mukherjee, S., Mahato, S., & Chavhan, S. (2019). Structural Features of Kinwat Peninsular Gneissic Complex Along the Western Margin of Eastern Dharwar Craton, India. Arabian Journal for Science and Engineering, 44, 6509-6523. https://doi.org/10.1007/s13369-019-03948-x
[13] Kaplay, R. D., Kumar, T. V., & Sawant, R. (2014). Field evidence for deformation in Deccan Traps in microseismically active Nanded area, Maharashtra. Current Science, 105(8).
[14] Kaplay, R. D., Kumar, T. V., Mukherjee, S., Wesanekar, P. R., Babar, M., & Chavan, S. (2017b). E-W strike slip shearing of Kinwat granitoid at South East Deccan Volcanic Province, Kinwat, Maharashtra, India. Journal of Earth System Science, 126(5), 71. https://doi.org/10.1007/s12040-017-0853-8.
[15] Kaplay, R. D., Vijay Kumar, T., & Sawant, R. (2013). Field evidence for deformation in Deccan Traps in microseismically active Nanded area, Maharashtra. Current Science, 105, 1051–1052.
[16] Keller, E. A., & Pinter, N. (1996). Active Tectonics, Upper Saddle River. *NJ: Prentice Hall*, *19*, 359.
[17] Melton MA (1958) Geometric properties of mature drainage systems and their representation in an E4 phase space. The Journal of Geology 66(1):35–54. https://doi.org/10.1086/626481
[18] Molin P, Pazzaglia F J and Dramis F (2004) Geomorphic expression of active tectonics in a rapidly-deforming forearc, Sila Massif, Calabria, southern Italy; Am. J. Sci. 304 559–589. https://doi.org/10.2475/ajs.304.7.559
[19] Ngapna, M. N., Owona, S., Owono, F. M., Mpesse, J. E., Youmen, D., Lissom, J., ... & Ekodeck, G. E. (2018). Tectonics, lithology and climate controls of morphometric parameters of the Edea-Eseka region (SW Cameroon, Central Africa): Implications on equatorial rivers and landforms. Journal of African Earth Sciences, 138, 219-232. https://doi.org/10.1016/j.jafrearsci.2017.11.008
[20] Pati, J. K., Lal, J., Prakash, K., & Bhusan, R. (2008). Spatio-temporal shift of western bank of the Ganga River, Allahabad city and its implications. Journal of the Indian Society of Remote Sensing, 36, 289-297. https://doi.org/10.1007/s12524-008-0030-2
[21] Prakash, K., Mohanty, T., Pati, J. K., Singh, S., & Chaubey, K. (2017). Morphotectonics of the Jamini River basin, Bundelkhand Craton, Central India; using remote sensing and GIS technique. Applied Water Science, 7, 3767-3782. https://doi.org/10.1007/s13201-016-0524-y.
[22] Radhakrishna, B.P. (1992) Cauvery – Its geological past. Jour. Geol. Soc. India. https://doi.org/10.17491/jgsi/1992/400101
[23] Rawat, A., Banerjee, S., Sundriyal, Y., & Rana, V. (2022). An integrated assessment of the geomorphic evolution of the Garhwal synform: Implications for the relative tectonic activity in the southern part of the Garhwal Himalaya. Journal of Earth System Science, 131(1), 56. https://doi.org/10.1007/s12040-021-01794-w
[24] Ritter, D.F. (1986) Process geomorphology, 2nd ed Wm. C. Brown Publishers.
[25] Sangode, S. J., Meshram, D. C., Kulkarni, Y. R., Gudadhe, S. S., Malpe, D. B., & Herlekar, M. A. (2013). Neotectonic response of the Godavari and Kaddam rivers in Andhra Pradesh, India: Implications to quaternary reactivation of old fracture system. Journal of the Geological Society of India, 81(4), 459-471. https://doi.org/10.1007/s12594-013-0062-2
[26] Schumm, S.A. (1956). The evolution of drainage systems and slopes in bad lands at Perth, Amboi, New Jersey. Geol. Soc. Ame. Bull. 67 (5), pp. 597_646. https://doi.org/10.1130/0016-7606(1956)67[597:EODSAS]2.0.CO;2
[27] Singh CP (2002) Applied geomorphology: a study. B. R. Publishing Corporation, Delhi.
[28] Singh, C. K. (2014). Active deformations extracted from drainage geomorphology: a case study from Southern Sonbhadra District, Central India. Journal of the Geological Society of India, 84, 569-578. https://doi.org/10.1007/s12594-014-0164-5
[29] Singh, C. K., & Srivastava, V. (2011). Morphotectonics of the Area around Renukoot, district Sonbhadra, UP using remote sensing and GIS techniques. Journal of the Indian Society of Remote Sensing, 39, 235-240. https://doi.org/10.1007/s12524-011-0072-8
[30] Sinha-Roy, S. (2001) Neotectonically controlled catchment capture: An example from the Banas and Chambal drainage basins Rajasthan. Curr. Sci., v.80, pp.293-298.
[31] Strahler, A. N. (1964). Quantitative geomorphology of drainage basin and channel networks. Handbook of applied hydrology.
[32] Twidale, C. R. (2004). River patterns and their meaning. Earth-Science Reviews, 67(3-4), 159-218.v.40, pp.1-12. https://doi.org/10.1016/j.earscirev.2004.03.001
[33] Villela, S. M., & Mattos, A. (1975). Hidrologia aplicada. Editora McGraw-Hill do Brasil.